www.czasopisma.pan.pl PAN POLSKA AKADEMIA NAUK www.journals.pan.pl

Arch. Metall. Mater. **68** (2023), 1, 5-13

DOI: https://doi.org/10.24425/amm.2023.141465

YADI FU[1], XUEYU DAI[2], HUIDI ZHANG[2], YIMIN WANG[1*]

ANTI-SEISMIC BEHAVIOR OF WELDED BOX SECTION COLUMN CONSIDERING WELDING RESIDUAL STRESS AT HIGH TEMPERATURE

To study the anti-seismic performance of steel structure under high temperature, the finite element analysis software ABAQUS was used to study the seismic performance of Q235 steel welded box section column at service stage under normal temperature and high temperature fire. The effects of welding residual stress, slenderness ratio, width thickness ratio and axial load level on the hysteretic behavior of columns were analyzed and the stable bearing capacity and hysteretic performance of the column under high temperature were investigated. The results show that the maximum bearing capacity of the column decreases with the increase of the residual stress peak value. With the increase of temperature, a decrease in the maximum bearing capacity of columns under constant axial force and horizontal cyclic load and an increase in the ductility occur.

Keywords: box section; high temperature; residual stress, hysteretic behavior

1. Introduction

Steel is more and more widely used in building structures due to its multitudinous advantages such as good plasticity, high strength and light weight. The good ductility and energy dissipation capacity of a steel structure make it have excellent seismic performance, but the local failure and collapse of a steel structure under strong earthquake are still common. Many areas of China are seriously affected by earthquake disasters, steel structure members and the whole structure may both lose stability under strong earthquake, resulting in structural damage and collapse [1]. Earthquake fire is the most important and serious secondary disaster caused by an earthquake, which often causes serious casualties and property losses. At the same time, steel is not a fire-resistant material, and fire not only affects the distribution of residual stress, but also reduces the components' long-term bearing capability after the fire.

Many academics have conducted studies on bearing capacity after the high temperature and seismic performance under room temperature of steel members.

Li and Shen [2] studied the ultimate bearing capacity of axially compressed steel members at high temperature and a simplified calculation method is proposed. Chen et al. [3] studied the influence of width to thickness ratio, slenderness ratio and residual stress on the performance of H-type fire-resistant steel column by loading the steel column to the ultimate state by specifying the temperature and proposed the design principle of fire-resistant steel column; Zhang [4] carried out axial compression test of Q690 steel I-section column after the high temperature, conducted numerical simulation and a large number of parameter analysis and introduced stability checking parameters after the fire, which provided reference for engineering application.

Fukumoto et al. [5] figured out the hysteretic behavior of short square steel tubular stub columns under uniaxial tensile cyclic loading through experiments. Kuwamura [6] studied the hysteretic behavior of high-strength steel compression-flexure members through reciprocating loading tests and found that the ductility of members with low yield ratio is better. Gao et al. [7,8] studied the correlation between ultimate strength and ductility of axial and eccentric compression steel columns under horizontal cyclic loading and the finite element formula of hysteretic behavior of steel column, considering geometric nonlinearity and material nonlinearity, is established. Hu et al. [9-11] analyzed the hysteretic behavior of Q235 steel I-section eccentrically loaded steel columns and put forward the limit values of axial compression ratio, slenderness ratio, width to thickness ratio and height to thickness ratio. Nakashima [12] carried out cyclic loading tests on six square steel tubular columns and conducted finite

[1] BEIJING CONSTRUCTION ENGINEERING GROUP CO. LTD, BEIJING, CHINA
[2] DEPARTMENT OF CIVIL ENGINEERING, CHINA AGRICULTURAL UNIVERSITY, BEIJING, CHINA
* Corresponding email: China4909@126.com

element analysis. Through numerical simulation, Liu [13] studied the hysteretic behavior of box section members and proposed the limit value of width to thickness ratio of a frame column.

There are currently just a few investigations on the seismic behavior of steel constructions under fire and high temperature, especially when considering welding residual stress under working condition. Therefore, it has far-reaching engineering significance to explore the seismic behavior of steel members in high-temperature environments.

In this paper, firstly, the impacts of slenderness ratio, width to thickness ratio and axial load level on the hysteretic behavior of Q235 steel welded box section columns are analyzed by ABAQUS. Then, the hysteretic behavior of Q235 steel welded box section column was studied and the impact of fire high temperature on the bearing capacity and ductility of members was analyzed as well. This provided a foundation for the mechanical performance study and structural design of steel structure under the high temperature and earthquake at the same time.

2. Finite element model

2.1. Model establishment

ABAQUS was employed to establish Q235 box section steel column model selecting C3D8R element. The steel column section measures 200 mm in height, 200 mm in width, 8 mm in plate thickness, and 2 m in length. The cross section of box section column is shown in Fig. 1(a). Along the section thickness direction, three elements are divided, and 30 elements with a length of around 67 mm are divided along the column length direction to increase computation accuracy and save time and cost.

The von Mises flow rule provided in ABAQUS is adopted for steel and the constitutive model is a combined one considering the strengthening part of isotropic model and nonlinear follow-up strengthening part of follow-up strengthening model. The parameters required for the constitutive model are recommended by Shi [14] for Q235 steel.

Furthermore, ABAQUS was used to simulate the welding process of the column. From the results represented in Fig. 1(b), it can be found that the maximum tensile stress of the section reaches 306 MPa and the maximum compressive stress is –72 MPa.

The column is constrained by the fixed end at the bottom and the top of the column is a cantilever free end. The model is loaded in three steps: (1) The residual stress obtained from simulation of a welding process is imported in the form of predefined field; (2) A fixed axial load is applied on the column top, meanwhile the axial compression ratio is set as 0.3; (3) The horizontal cyclic load is applied on the column top by displacement loading. According to the provisions on the limit of inter story displacement angle in reference [15], the displacement loading system is $\pm L/300$, $\pm L/150$, $\pm L/100$, $\pm L/80$, $\pm L/70$, $\pm L/60$, $\pm L/50$, $\pm L/40$, $\pm L/30$.

2.2. Model verification

Fig. 2 plots the hysteretic curve of the column under the action of constant axial force and horizontal cyclic load obtained by finite element analysis, in which the abscissa represents the horizontal displacement of the free end of the column, and the ordinate represents the horizontal load at the free end of the column. The hysteretic curve of the column in Fig. 2 is relatively plump and Q235 welded box section steel column shows good hysteretic performance.

The maximum value of the hysteretic curve at each loading cycle stage is extracted to form the skeleton curve, as depicted in Fig. 3. In the initial stage of loading, the load increases linearly with the displacement. When the top of the column moves to the left or right by about 40mm, the load is roughly unchanged, the horizontal displacement continues to increase and the curve of the component appears a platform section. At this time, it can be judged that the column is damaged. The curves in Fig. 2 and Fig. 3 are roughly consistent with those measured by Li et al. [16], indicating the accuracy of the model

3. Results and discussion

3.1. Effects of parameters on the column hysteretic performance

The influence of slenderness ratio, width to thickness ratio, residual stress and axial load level on the hysteretic performance of welded box section steel column under working condition is

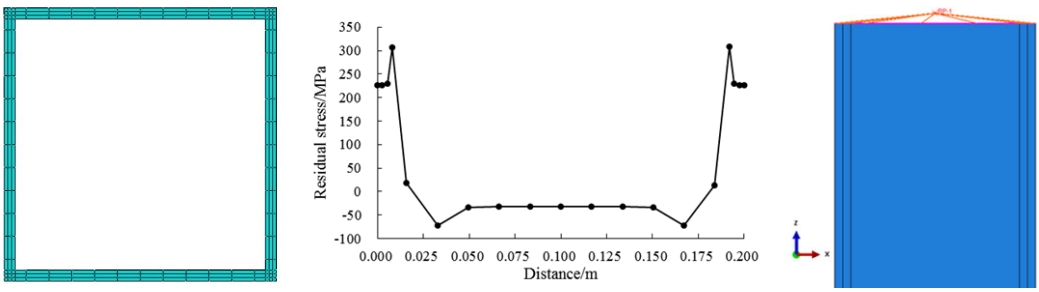

(a) (b) (c)

Fig. 1. Finite element model setting diagram: (a) Mesh generation of model section from the top view of column, (b) Residual stress distribution of section, (c) Boundary condition

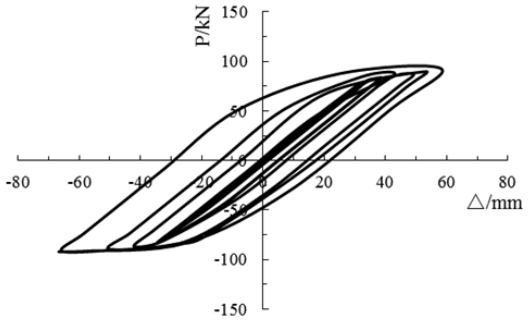

Fig. 2. Hysteretic curve

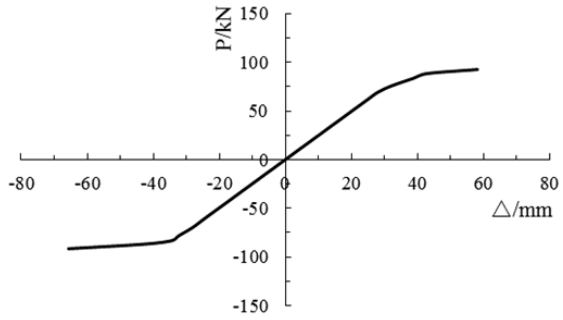

Fig. 3. Skeleton curve

analyzed. Finally, the hysteretic performance analysis considering the high temperature is carried out under the condition of better bearing capacity and hysteretic performance.

TABLE 1

List of slenderness ratio calculation examples

Column number	λ	L/mm	b_0/mm	t/mm	Axial compression ratio
B20-25-0.3	20	800	200	8	0.3
B30-25-0.3	30	1200	200	8	0.3
B40-25-0.3	40	1600	200	8	0.3
B50-25-0.3	50	2000	200	8	0.3

According to the limit value of slenderness ratio of a frame column in reference [17] and reference [15], four slenderness ratios are selected for parameter analysis in this paper: $\lambda = 20$, 30, 40 and 50. The column number and size are shown in TABLE 1, where the numbers in column number represents the slenderness ratio, width to thickness ratio and axial compression ratio of the column, respectively, L represents the member length, b_0 represents the section width of the equilateral box section and t represents section thickness of the equilateral box section.

Fig. 4 illustrates the hysteretic curves of the column with slenderness ratio of 20. Comparing the hysteretic curves of the columns with different slenderness ratios, when λ = 20, 30, 40 and 50, the hysteretic curves of the members are close to the parallelogram, the hysteretic curves are plump and the columns are good at energy dissipation. It is obvious to figure out that the plumpness of hysteretic curve decreases with the increase of slenderness ratio, furthermore, the maximum load capacity goes down as the slenderness ratio goes up.

Fig. 5 plots the skeleton curve of each column, which shows that the initial elastic stiffness and maximum bearing capacity of B50-25-0.3 are the smallest and the column stiffness gradually decreases when slenderness ratio is increasing. The maximum bearing capacity of specimen B30-25-0.3 is slightly lower than that of specimen B40-25-0.3 and the maximum bearing capacity of other specimens decreases when slenderness ratio increases . Besides, when the slenderness ratio gets smaller, the degradation rate of bearing capacity becomes faster.

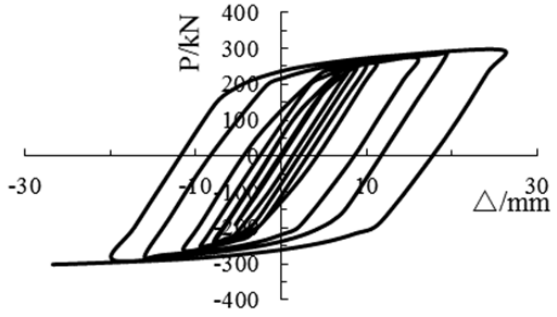

Fig. 4 B20-25-0.3 hysteretic curve

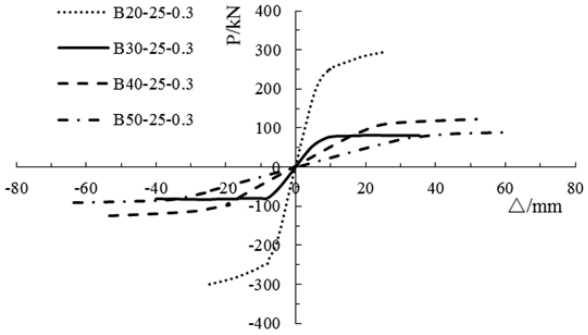

Fig. 5 Skeleton curves of members

Width to thickness ratio of plate not only exerts a tremendous impact on the seismic performance of steel structure, but also determines the steel consumption of steel structure, which is greatly significant to the safety and economy of steel structure. According to specifications, five ratios of width to thickness are selected for parameter analysis in this paper, b_0/t are 19, 23, 25, 27 and 31, respectively. For the examples, the number and size of components are revealed in TABLE 2.

TABLE 2

List of width to thickness ratio calculation examples

Column number	L/mm	b_0/mm	t/mm	b_0/t	λ
B50-19-0.3	2000	152	8	19	68
B50-23-0.3	2000	184	8	23	56
B50-25-0.3	2000	200	8	25	51
B50-27-0.3	2000	216	8	27	47
B50-31-0.3	2000	248	8	31	41

Fig. 6 depicts the hysteretic curve of the column with the width to thickness ratio of 31. When the width to thickness ratio

of a column is 19, the plumpness of the hysteretic curve is low, while when the ratio of width to thickness is 23, 25, 27 and 31, the hysteretic curves are close to parallelogram without an obvious pinch phenomenon, and the plump curves indicate that the columns possess desired energy dissipation capacity. The maximum bearing capacity increases with increase of width to thickness ratio.

In Fig. 7, the skeleton curves of all columns indicates that the initial elastic stiffness of the column increases as the width to thickness ratio increasing. More load can be supported by a surface if the ratio of its width to thickness becomes larger. This is because when the thickness of the plate remains unchanged, larger width to thickness ratio generates larger section width. If the column possesses larger width to thickness ratio, faster degradation rate of the bearing capacity and smaller horizontal displacement of the column top will occur.

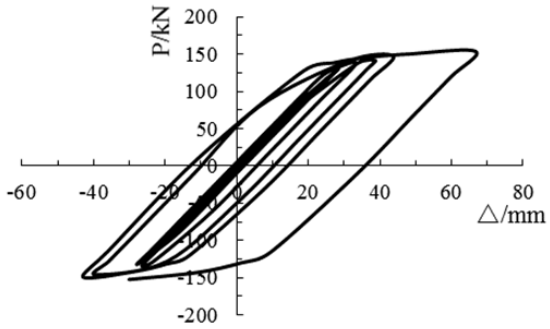

Fig. 6. Hysteretic curve of B50-31-0.3

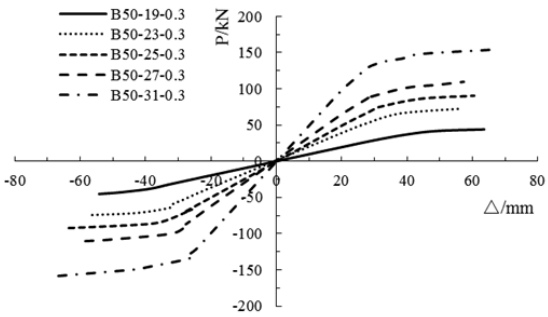

Fig. 7. Skeleton curves of columns

TABLE 3

Residual stress calculation examples

Column number	L/mm	b_0/mm	t/mm	Peak tensile stress /MPa	Peak tensile stress /MPa
B50-25-1	2000	200	8	0	0
B50-25-2	2000	200	8	306	–72
B50-25-3	2000	200	8	449	–129

To consider how the residual stress affects the columns' hysteretic behavior, the parameter analysis of residual stress is carried out. Without changing the distribution mode of residual stress, only the magnitude of residual stress is changed. Fig. 8 plots the residual stress distribution of different residual stress examples, and TABLE 3 lists the values of the peak residual tensile stress and peak residual compressive stress.

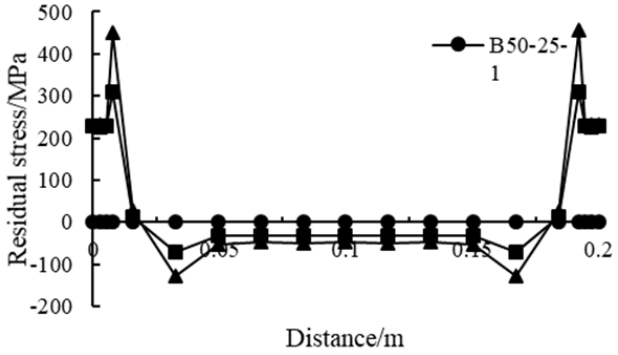

Fig. 8. Residual stress distribution of calculation example

The hysteretic curves and the skeleton curves of the column in the case of variable residual stress are illustrated in Fig. 9 and Fig. 10. The hysteretic curves of the columns in the case of residual stress and no residual stress are all relatively plump, showing good energy dissipation performance of Q235 welded box section steel columns. When considering the residual stress, the maximum bearing capacity is smaller than that of the column without residual stress, mainly because the residual stress makes the weld zone of the column yield in advance. When the residual stress changes, the skeleton curves of the columns roughly coincide. The maximum bearing capacity of columns B50-25-1, B50-25-2 and B50-25-3 are 88.4 kN, 85.6 kN and

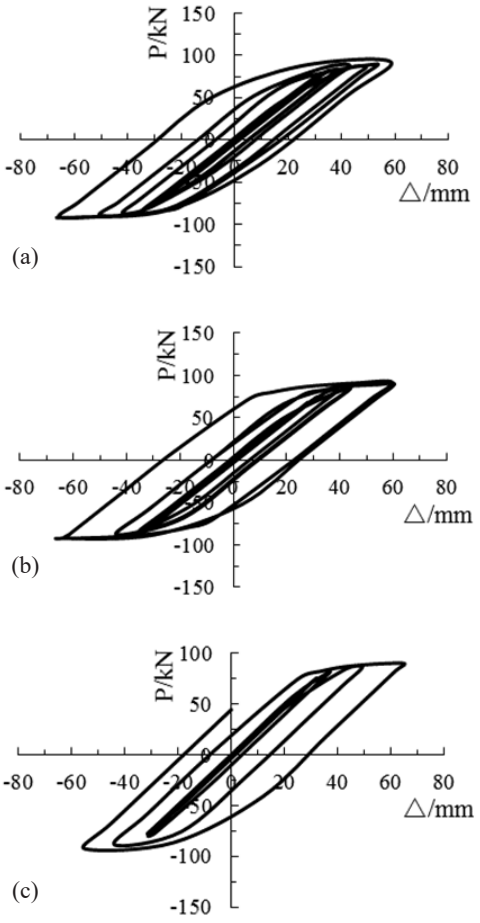

Fig. 9. Hysteretic curves of members: (a) B50-25-1, (b) B50-25-2, (c) B50-25-3

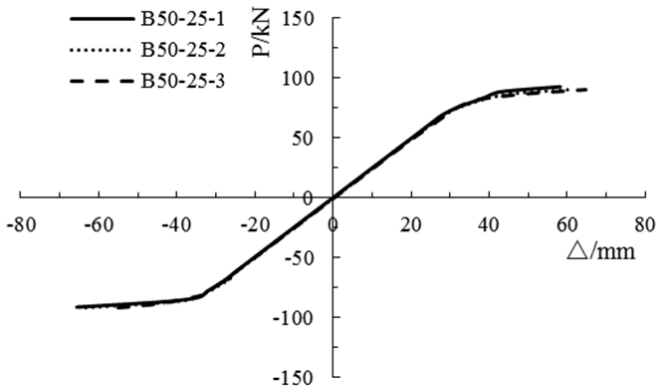

Fig. 10. Load-displacement skeleton curves of members

81.5 kN, respectively, with a slight decrease by 3.17% and 7.81% respectively, and it can be inferred that the declining range of maximum bearing capacity increases with the increase of residual stress peak.

The axial load level N/Af_y significantly affects the second-order effect of the column and a larger axial compression ratio will make the column reach the yield state or local instability, so it is necessary to analyze the axial load level parameters of the column under the horizontal cyclic load. Considering the stress condition of the compression bending member in the actual project, the axial compression ratio is 0, 0.2, 0.3, 0.4 and 0.6 in the parameter analysis of this paper. The number and size of the column are shown in TABLE 4 in the calculation example analysis.

TABLE 4

List of axial load level calculation examples

Column number	L/mm	b_0/mm	t/mm	b_0/t	N/Af_y
B50-19-0	2000	152	8	19	0
B50-19-0.2	2000	152	8	19	0.2
B50-19-0.3	2000	152	8	19	0.3
B50-19-0.4	2000	152	8	19	0.4
B50-19-0.6	2000	152	8	19	0.6
B50-23-0	2000	184	8	23	0
B50-23-0.2	2000	184	8	23	0.2
B50-23-0.3	2000	184	8	23	0.3
B50-23-0.4	2000	184	8	23	0.4
B50-23-0.6	2000	184	8	23	0.6
B50-25-0	2000	200	8	25	0
B50-25-0.2	2000	200	8	25	0.2
B50-25-0.3	2000	200	8	25	0.3
B50-25-0.4	2000	200	8	25	0.4
B50-25-0.6	2000	200	8	25	0.6
B50-27-0	2000	216	8	27	0
B50-27-0.2	2000	216	8	27	0.2
B50-27-0.3	2000	216	8	27	0.3
B50-27-0.4	2000	216	8	27	0.4
B50-27-0.6	2000	216	8	27	0.6
B50-31-0	2000	248	8	31	0
B50-31-0.2	2000	248	8	31	0.2
B50-31-0.3	2000	248	8	31	0.3
B50-31-0.4	2000	248	8	31	0.4
B50-31-0.6	2000	248	8	31	0.6

Fig. 11 shows the hysteretic curves of some columns when width to thickness ratio is 19, Fig. 12 shows the load-displacement skeleton curves of columns with a width to thickness ratio of 23, 27 and 31. According to the hysteretic curves of columns in TABLE 4, when width thickness to ratio is fixed and the axial compression ratio changes, the shape of the hysteretic curves of the columns is roughly the same. As the axial compression ratio increases, the maximum bearing capacity and ductility of the column decrease.

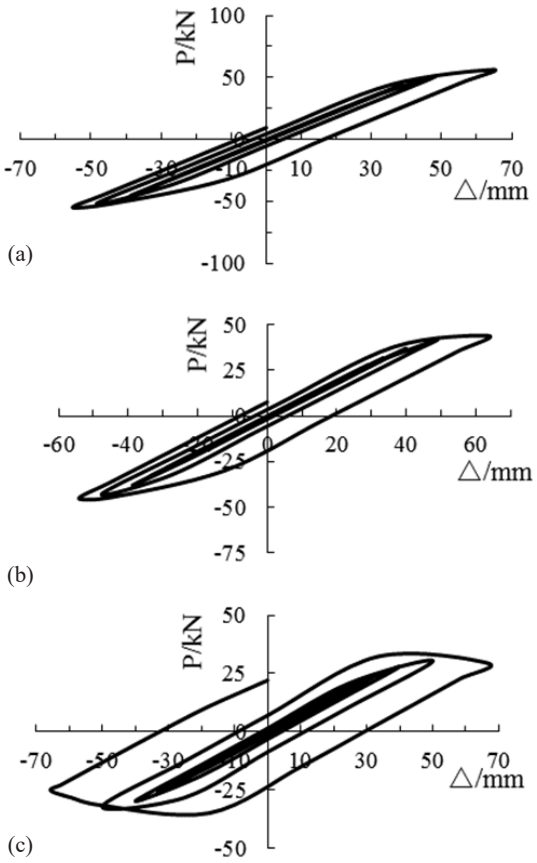

Fig. 11. Hysteretic curves of the columns with a width to thickness ratio of 19: (a) $N/Af_y = 0$, (b) $N/Af_y = 0.3$, (c) $N/Af_y = 0.6$

According to the skeleton curve of columns in TABLE 4, when the axial compression ratio increases, without modifying the width to thickness ratio, the maximum value of the load-displacement skeleton curve decreases, that is, the maximum bearing capacity of the column decreases, and the bearing capacity degradation is faster as well. The horizontal displacement decreases gradually when the bearing capacity reaches the maximum or tends to be flat and the ductility of the column becomes worse as the axial compression ratio increases.

The column with good bearing capacity and hysteresis performance is selected for the hysteretic performance analysis considering the high temperature action. The material parameters of steel at high temperature are taken according to European Code EC3 [18] and the steel constitutive model is consistent with Section 2. ISO834 standard temperature rising curve [19] is used to figure out how the temperature of the environment

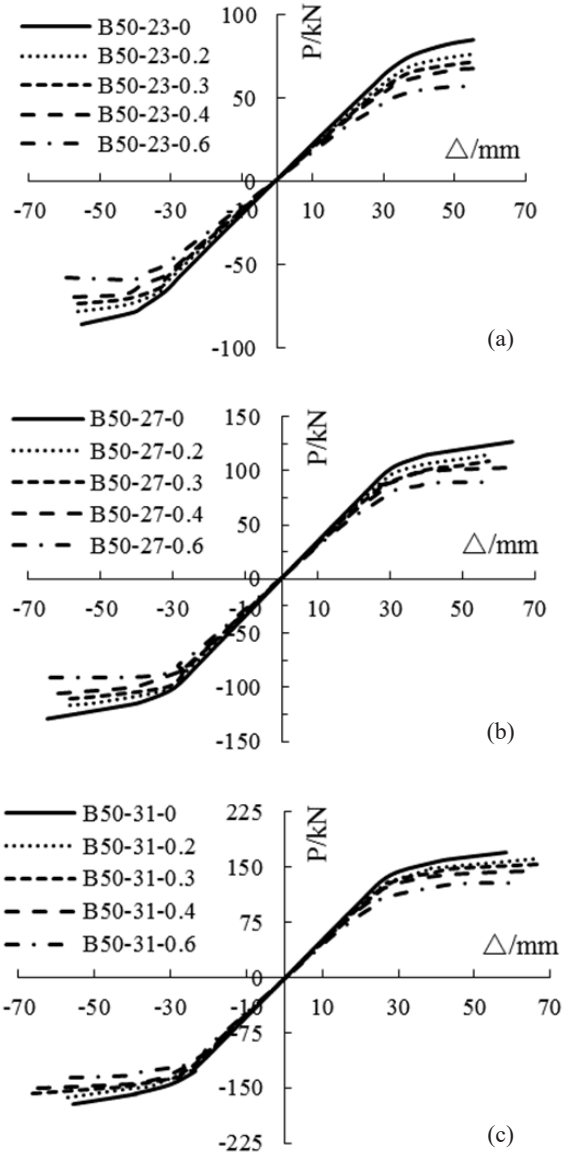

Fig. 12. Skeleton curves of columns: (a) b_0/t = 23, (b) b_0/t = 27, (c) b_0/t = 31

changes. Fire is coming at the steel column from all four sides, making the steel column heating unevenly, so the column top and bottom are set as non-fire surfaces and the thermal radiation condition is defined. The rest boundary is set as the fire surface, which defines the heat convection and thermal radiation conditions and assumes that the thermal boundary conditions of steel column are not affected by structural deformation.

Considering the temperature of the column, the main parameters of the high temperature hysteresis performance analysis are selected. In this paper, the axial pressure ratio is 0.3 and the width to thickness ratio is 23, 25 and 27, respectively. When analyzing the examples, the number and size of the columns are shown in TABLE 5.

Fig. 13 shows that the shape of the skeleton curves of the columns is roughly unchanged, but with the increase of fire temperature, the skeleton curve of the column gradually decreases, that is, the maximum bearing capacity of the column decreases. At 500°C and 600°C, the bearing capacity decreases greatly.

TABLE 5

List of the high temperature calculation examples

Column number	L/mm	b_0/mm	t/mm	b_0/t	N/Af_y	Temperature /°C
B50-23-20	2000	184	8	23	0.3	20
B50-23-300	2000	184	8	23	0.3	300
B50-23-400	2000	184	8	23	0.3	400
B50-23-500	2000	184	8	23	0.3	500
B50-23-600	2000	184	8	23	0.3	600
B50-25-20	2000	200	8	25	0.3	20
B50-25-300	2000	200	8	25	0.3	300
B50-25-400	2000	200	8	25	0.3	400
B50-25-500	2000	200	8	25	0.3	500
B50-25-600	2000	200	8	25	0.3	600
B50-27-20	2000	216	8	27	0.3	20
B50-27-300	2000	216	8	27	0.3	300
B50-27-400	2000	216	8	27	0.3	400
B50-27-500	2000	216	8	27	0.3	500
B50-27-600	2000	216	8	27	0.3	600

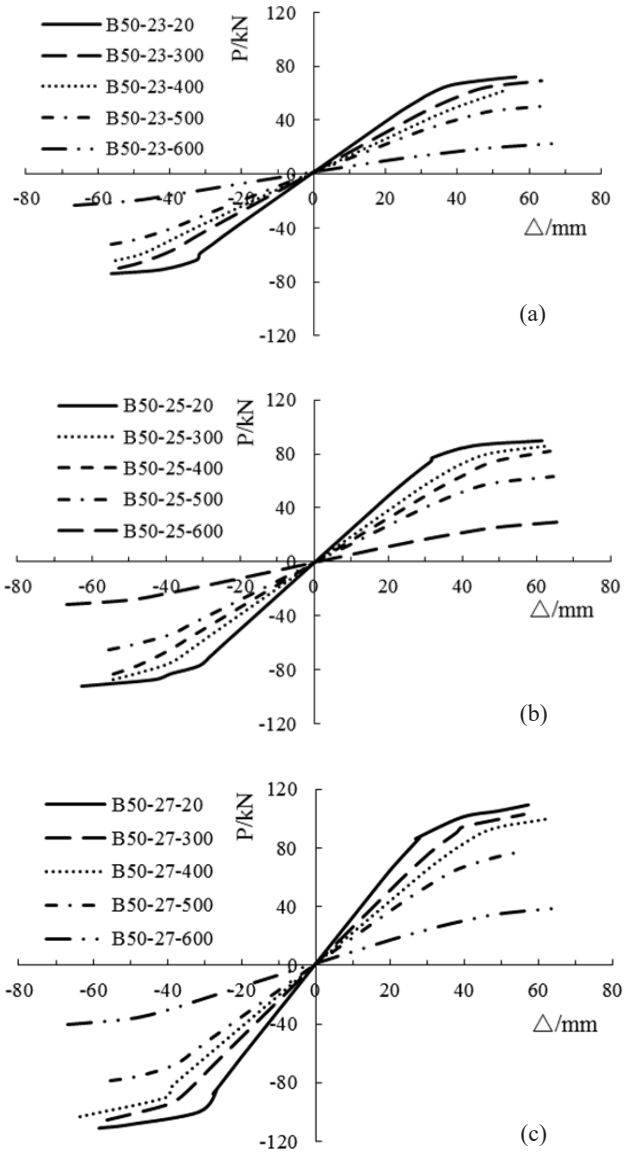

Fig. 13. Skeleton curves of specimens under high temperature: (a) b_0/t = 23, (b) b_0/t = 25, (c) b_0/t = 27

3.2 The hysteretic performance evaluation

In this paper, the hysteretic behavior of the column under normal axial force and horizontal cyclic load is quantitatively evaluated from the two aspects of bearing capacity reduction and ductility.

Reference [15] stipulates that the elastic-plastic inter story displacement angle of multi-story and high-rise steel structures is limited to 1/50. To study how columns behave when a constant axial force and a cyclic horizontal load are applied, the bending moment $M_{0.02}$ is defined, that is, the corresponding bending moment when the elastic-plastic displacement angle reaches $L/50$; The bending moment M_u is the bending moment corresponding to the peak of the skeleton curve. $M_{0.02}/M_u$ can reflect the reduction of the bearing capacity of the column when the elastic-plastic displacement angle reaches the limit value specified in the code. The relationship between plate width to thickness ratio, axial compression ratio and bearing capacity reduction range in TABLE 4 is shown in Fig. 14, and the specific values of bearing capacity reduction range are shown in TABLE 6.

Fig. 14 shows that as the axial compression ratio remains unchanged, the width to thickness ratio of the plate is less than 31, the value of $M_{0.02}/M_u$ of the columns is greater than 0.75, reflecting good bearing capacity. When the plate width to thickness ratio is 19, 23, 25, and the axial compression ratio is 0, 0.2, 0.3, 0.4, the value of $M_{0.02}/M_u$ increases with increase of the width to thickness ratio, reflecting better bearing capacity of the column. When the plate width to thickness ratio is 31 and the axial compression ratio is 0, 0.2 and 0.3, the value of $M_{0.02}/M_u$ is 0.92, which indicates that the plate width to thickness ratio is the main variable influencing the bearing capacity of the column under this condition and the bearing capacity of is better in the case. When the plate width to thickness ratio is 31 and the axial compression ratio is 0.4 and 0.6, $M_{0.02}/M_u$ equals 0.69 and 0.75, respectively, indicating a great decrease in the bearing capacity of the column and worse bearing capacity.

As the axial pressure ratio is 0.2 and 0.3, the columns still have good bearing performance after reaching the limit of displacement angle between plastic layers specified in the specification and can be used in design. When the axial pressure ratio is 0.4, 0.6 and the width to thickness ratio is 31, the bearing capacity of the column drops suddenly and the bearing performance of the column is unstable.

TABLE 6

Calculation results of quantitative evaluation of hysteresis performance

Column number	b_0/t	N/Af_y	$M_{0.02}/M_u$	μ
B50-19-0	19	0	0.785	3.300
B50-19-0.2	19	0.2	0.809	2.814
B50-19-0.3	19	0.3	0.832	2.543
B50-19-0.4	19	0.4	0.851	1.969
B50-19-0.6	19	0.6	0.870	1.600
B50-23-0	23	0	0.892	4.962
B50-23-0.2	23	0.2	0.933	3.300
B50-23-0.3	23	0.3	0.940	2.814
B50-23-0.4	23	0.4	0.968	2.109
B50-23-0.6	23	0.6	0.950	1.367
B50-25-0	25	0	0.934	4.962
B50-25-0.2	25	0.2	0.948	3.880
B50-25-0.3	25	0.3	0.967	3.074
B50-25-0.4	25	0.4	0.974	2.032
B50-25-0.6	25	0.6	0.952	1.656
B50-27-0	27	0	0.908	4.962
B50-27-0.2	27	0.2	0.922	4.310
B50-27-0.3	27	0.3	0.922	3.370
B50-27-0.4	27	0.4	0.985	1.980
B50-27-0.6	27	0.6	0.926	1.511
B50-31-0	31	0	0.921	4.962
B50-31-0.2	31	0.2	0.919	4.937
B50-31-0.3	31	0.3	0.921	3.065
B50-31-0.4	31	0.4	0.692	1.868
B50-31-0.6	31	0.6	0.753	1.615

To analyze the hysteretic behavior of columns, the ductility coefficient μ is defined as

$$\mu = \frac{\delta_u}{\delta_y} \tag{1}$$

where δ_u is the top horizontal displacement of the column when the column reaches failure, δ_y is the top horizontal displacement of the column when the edge of the column enters the yield state.

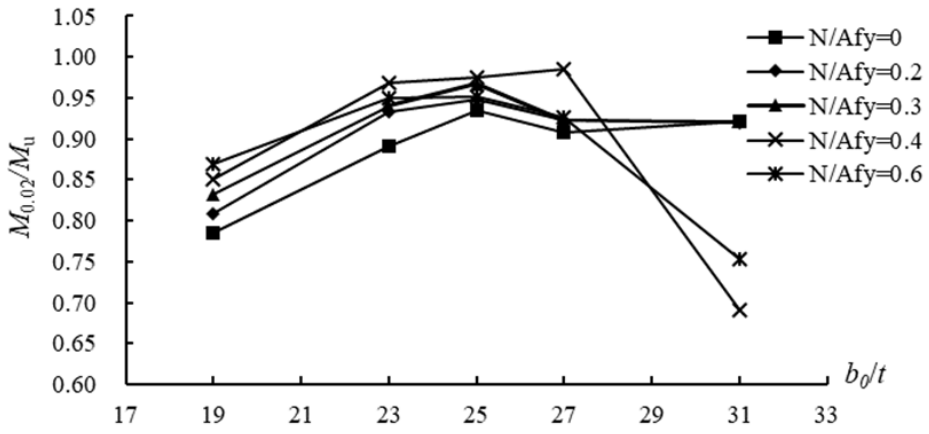

Fig. 14. b_0/t – $M_{0.02}/M_u$ curve

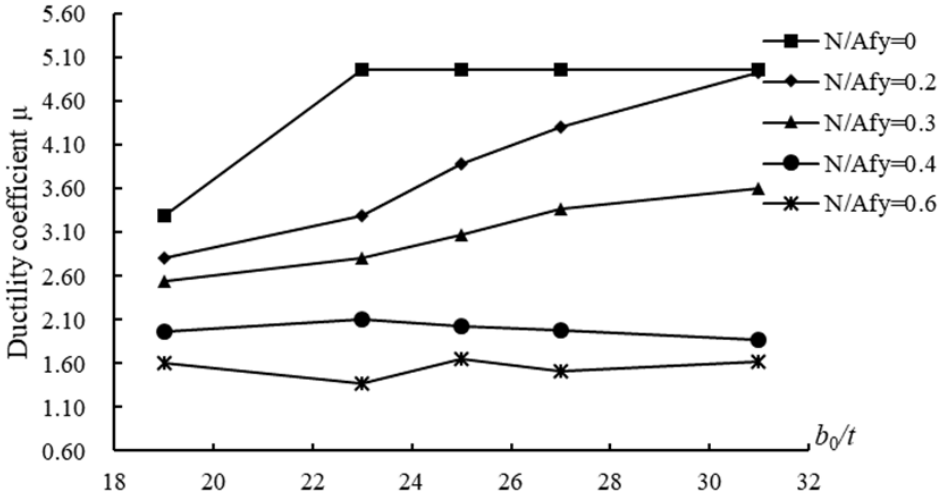

Fig. 15. $b_0/t - \mu$ curve

The relationship between the width to thickness ratio of the plate, axial compression ratio and ductility coefficient in TABLE 4 is depicted in Fig. 15 and the specific values of ductility coefficient are plotted in TABLE 6.

Fig. 15 shows that the smaller the axial compression ratio is, the greater the ductility coefficient is and thus the better the ductility performance of the column is, with the width to thickness ratio unchanged. When N/Af_y is 0 and the width to thickness ratio is 23, 25, 27 and 31, the ductility coefficient is 4.96. When N/Af_y is 0.2 and 0.3, the ductility coefficient increases when increasing the width to thickness ratio and the ductility performance of the column is better. When N/Af_y is 0.4 and 0.6, the ductility coefficient is less than 2.1 with little variation with the width thickness ratio, hence, the ductility performance gets poor, which indicates that higher axial load level will reduce the ductility of the column.

To figure out how high temperature of fire affects the hysteretic behavior of columns, the reduction coefficient of bearing capacity under the high temperature is defined as

$$\varphi_T = \frac{F_{uT}}{F_u} \tag{2}$$

where F_{uT} is the load corresponding to the highest point of skeleton curve at high temperature, F_u is the load corresponding to the highest point of skeleton curve at room temperature.

To quantitatively evaluate the ductility performance of columns under constant axial force and horizontal cyclic load under high temperature, the ductility coefficient under the high temperature is defined as

$$\varphi_T = \frac{\delta_{uT}}{\delta_{yT}} \tag{3}$$

where δ_{uT} is the top horizontal displacement of the column when the column reaches failure at high temperature, δ_{yT} is the top horizontal displacement of the column when the edge of the column enters the yield state at high temperature.

The bearing capacity reduction coefficient and ductility coefficient in TABLE 5 are shown in TABLE 7. The bearing capacity reduction coefficient decreases with the increase of temperature. The bearing capacity reduction coefficient does not change much at 300°C and 400°C, whereas the reduction in bearing capacity gets worse at 500°C and 600°C. When the heat level is 600°C, The bearing capacity reduction coefficient s of B50-23-600, B50-25-600 and B50-27-600 are 0.32, 0.33 and 0.36, respectively, indicating that high temperature weakens the bearing capacity notably. In terms of the ductility coefficient of the column, when the temperature is 20°C, 300°C and 400°C, it does not change much, while at 500°C and 600°C, the ductility coefficient of the column increases, especially at 600°C, it increases about 700% compared to that at normal temperature.

TABLE 7

Reduction coefficient of bearing capacity at high temperature

Column number	b_0/t	N/Af_y	Temperature/°C	φ_T	μ_T
B50-23-20	23	0.3	20	/	2.38
B50-23-300	23	0.3	300	0.92	2.54
B50-23-400	23	0.3	400	0.90	2.17
B50-23-500	23	0.3	500	0.73	3.28
B50-23-600	23	0.3	600	0.32	19.91
B50-25-20	25	0.3	20	/	2.66
B50-25-300	25	0.3	300	0.96	3.18
B50-25-400	25	0.3	400	0.92	2.54
B50-25-500	25	0.3	500	0.71	3.23
B50-25-600	25	0.3	600	0.33	19.91
B50-27-20	27	0.3	20	/	2.46
B50-27-300	27	0.3	300	0.94	2.81
B50-27-400	27	0.3	400	0.91	2.50
B50-27-500	27	0.3	500	0.71	3.10
B50-27-600	27	0.3	600	0.36	19.91

4. Conclusions

The conclusions of this paper are as follows:

(1) The effects of slenderness ratio, width to thickness ratio, residual stress and axial load level on the hysteretic behavior

of the columns are studied. Larger slenderness ratio leads to smaller the maximum bearing capacity and slower degradation rate of the bearing capacity. Besides, larger width to thickness ratio leads to plumper hysteretic curve, greater maximum bearing capacity and faster bearing capacity degradation. Considering the residual stress, the maximum bearing capacity decreases and its decrease range rises up with increase of the peak value of the residual stress.

(2) When axial compression ratio is larger, smaller maximum bearing capacity and faster degradation rate of bearing capacity occur, meanwhile, the horizontal displacement declines gradually when the bearing capacity reaches the maximum or tends to be flat, and the ductility of the column becomes worse. When the axial compression ratio is 0.2 and 0.3, the column still possess desired bearing capacity after reaching the plastic interlayer displacement angle limit stipulated in the code, and the ductility coefficient increases when the width to thickness ratio gets larger which signifies good ductility. When the axial compression ratio is 0.6 and the width to thickness ratio is 23 or 31, the bearing capacity of the column drops suddenly and instability occurs. When the axial compression ratio is 0.4 and 0.6, the ductility coefficient is less than 2.1 which signifies poor ductility, indicating that higher axial load level reduces the ductility.

(3) The maximum bearing capacity of columns under horizontal cyclic load decreases as temperature rises. At 600°C, the bearing capacity is weakened significantly by high temperature. Below 400°C, the ductility coefficient changes little, while at 500°C and 600°C, the ductility coefficient increases, especially at 600°C, it increases by about 700% compared to that at normal temperature.

REFERENCES

[1] G.Q. L, J. Li, X.Z. Su, Seismic Design of Building Structures, China Construction Industry Press, Beijing (2008).

[2] G.Q. Li, S.Y. Zu, Ultimate Bearing Capacity of Axially Compressed Steel Members Under High Temperature. Building Structure **09**, 23-25 (1993).
DOI: https://doi.org/10.19701/j.jzjg.1993.09.007

[3] K.C. Yang, H.H. Lee, O. Chan, Experimental Study of Fire-Resistant Steel H-Columns at Elevated Temperature. J. Constr. Steel. Res. **62** (6), 544-553 (2006).
DOI: https://doi.org/10.1016/j.jcsr.2005.09.008

[4] J. Zhang, Research on Residual Stress and Mechanical Behavior of High Strength Q690 Steel Welded Section Column After Fire. PhD thesis, Chongqing University, China (2019).

[5] Y. Fukumoto, H. Kusama, Local Instability Tests of Plate Elements Under Cyclic Uniaxial Loading. J. Struct. Eng. **111** (5), 1051-1067 (1985). DOI:
https://doi.org/10.1061/(ASCE)0733-9445(1985)111:5(1051)

[6] H. Kuwamura, B. Kato, Inelastic Behavior of High Strength Steel Members with Low Yield Ratio, in: Proc. of the Pacific Structural Steel Conference. N.S.W, Australian Institute of Steel Construction, Australia, 429-437 (1989).

[7] S.B. Gao, T. Usami, H. B. Ge, Eccentrically Loaded Steel Columns Under Cyclic In-Plane Loading. J. Struct. Eng. **126** (8), 964-973(2000). DOI:
https://doi.org/10.1061/(ASCE)0733-9445(2000)126:8(974)

[8] S.B. Gao, T. Usami, H.B. Ge, Eccentrically Loaded Steel Columns Under Cyclic Out-of-Plane Loading. J. Struct. Eng. **126** (8), 974-981 (2000). DOI:
https://doi.org/10.1061/(ASCE)0733-9445(2000)126:8(974)

[9] Z.T. Hu, Q. Gu, Research on Hysteretic Behavior of Eccentrically Compressed Members Under Cyclic Loading. Building Structure **02**, 10-12 (2002).
DOI: https://doi.org/10.19701/j.jzjg.2002.02.003

[10] Z.T. Hu, Nonlinear Bending Torsion Related Buckling of Steel Members Subjected to Cyclic Loading. PhD thesis, Xi'an University of Architecture and Technology, China (2001).

[11] Z.T. Hu, Q. Gu, Nonlinear Flexural Torsional Buckling of Compression Bending Members Under Cyclic Loading. J. Building Structures **23** (3), 14-18 (2002).
DOI: https://doi.org/10.3321/j.issn:1000-6869.2002.03.003

[12] M. Nakashima, D. Liu, Instability and Complete Failure of Steel Columns Subjected to Cyclic Loading. J. Eng. Mech. **131** (6), 559-567 (2005).
DOI: https://doi.org/10.1061/(ASCE)0733-9399(2005)131:6(559)

[13] T. Liu, Research on Stability Bearing Capacity and Hysteretic Behavior of Box Section Members. PhD thesis, Tsinghua University, China (2005).

[14] Y.J. Shi, M. Wang, Y.Q. Wang, Constitutive Model of Structural Steel Under Cyclic Loading. Eng. Mech. **29** (09), 92-98 (2012).
DOI: https://doi.org/10.6052/j.issn.1000-4750.2010.09.0711

[15] Ministry of housing and urban rural development of the people's Republic of China, Code for Seismic Design of Buildings GB 50011-2010, China Construction Industry Press, Beijing (2010).

[16] G.Q. Li, Y.B. Wang, S.W. Chen, W. Cui, F.F. Sun. Experimental Study on Q460C High Strength Structural Steel Welded H-Shaped and Box Section Columns Under Low Cyclic Loading. J. Building Structures **34** (03), 80-86 (2013).
DOI: https://doi.org/10.14006/j.jzjgxb.2013.03.007

[17] Ministry of housing and urban rural development of the people's Republic of China, Standard for Design of Steel Structures GB 50017-2017, China Construction Industry Press, Beijing (2018).

[18] European Committee for Standardization, ENV 1993-1-2 Eurocode 3: Design of Steel Structures-Part 1.2: Structural Fire Design, 1993.

[19] J. Jiang, S.P. Chiew, C.K. Lee, P.L.Y. Tiong, An Experimental Study on Residual Stresses of High Strength Steel Box Columns. J. Constr. Steel Res. **130** (2017).
DOI: https://doi.org/10.1016/j.jcsr.2016.11.025